Periodico di Mineralogia (2013), 82, 2, 239-250 DOI: 10.2451/2013PM0014

PERIODICO di MINERALOGIA
established in 1930

An International Journal of
MINERALOGY, CRYSTALLOGRAPHY, GEOCHEMISTRY, ORE DEPOSITS, PETROLOGY, VOLCANOLOGY
and applied topics on *Environment*, *Archaeometry* and *Cultural Heritage*

Characterization of Elephant and Mammoth Ivory by Solid State NMR

Silvia Bracco[1], Anna Brajkovic[2,*], Angiolina Comotti[1] and Vanda Rolandi[3,*]

[1]Department of Materials Science, University of Milano-Bicocca, Via R. Cozzi 53, 20125 Milano, Italy
[2]Department of Earth and Environmental Sciences, University of Milano-Bicocca, Piazza della Scienza 4, 20126 Milano, Italy
[3]Italian Gemmologists Association (CIG), Via F. Caracciolo 63, 20155 Milano, Italy
*Corresponding authors: *anna.brajkovic@unimib.it*; *vanda.rolandi@fastwebnet.it*

Abstract

Ivory has always been considered one of the most attractive and valuable biological gem materials. It is tooth dentin, or the yellowish white, calcified, extremely elastic tissue that forms the tusks of several mammalian species. Microscopic examination of the surface in all possible directions is needed to a successful identification of cut and polished samples of ivory, but sometimes it is not enough. Supplemental techniques should be used for assisting discrimination of elephant (both *Loxodonta africana* and *Elephas maximus*) ivory and wholly mammoth (*Mammuthus primigenius*) ivory, because from a textural standpoint they can be remarkably similar. To provide the key identifying features of these two types of ivory is nowadays of special significance, due to the fact that elephant ivory trade and import and export are illegal, whereas wholly mammoth tusks may be legally exported and manufactured. Both materials are formed primarily by nanocrystals of biological calcium orthophosphate that are embedded in a type I collagen matrix. By exploiting ^{1}H, ^{13}C and ^{31}P magic angle spinning (MAS) NMR we investigated the composition of several elephant and mammoth ivory specimens. ^{13}C MAS NMR spectra confirmed the presence of the CO_3^{2-} group associated to the carbonated hydroxyapatite in both ivory types. In the collagen structure no differences have been highlighted. Quantitative ^{31}P MAS NMR spectra revealed important features about the inorganic matrix. The high resolution allowed us to achieve the simultaneous detection of the signal assigned to the bulk PO_4^{3-} groups of the hydroxyapatite phase and of minor side peaks ascribed to unprotonated surface sites PO_x (PO, PO_2^- and PO_3^{2-}) and to protonated sites PO_xH on the surface of the nano-sized crystals of the hydroxyapatite.

Key words: ivory; elephant; mammoth; dentin; orthophosphate; MAS NMR.

Introduction

Ivory is a biological gem material, being derived from parts of animals. It is the product of the mineralization of the connective tissue in the tusks (or prominent teeth) of mammals. It is dentin or a calcified, extremely elastic tissue that forms the bulk of all mammalian teeth. In evolutionary terms, dentin is an older and less differentiated tissue than bone. Due to its warm creamy colour, good elasticity, resistance to fracture and easy to working and carving, ivory has been long considered to be a noble ornamental material to such an extent that it has been utilized from prehistory by virtually every civilization. Commercial sources of ivory would include the tusks of several mammals, but by tradition only elephantine ivory is termed simply "ivory". The other ivories should be identified by prefixing the name of their species of origin (e.g. mammoth ivory).

Elephant and mammoth ivory have similar surface features. Therefore it is sometimes quite difficult to discriminate between them, particularly if objects are of small size. Nevertheless identification is nowadays of special significance, due to the fact that elephant ivory trade and import and export are illegal. CITES, the Convention on International Trade in Endangered Species of Wild Fauna and Flora, in 1975 listed the Asian elephant and in 1989 the African elephant in Appendix I, the maximum level of protection to help safeguard from illegal killing (widespread hunting and poaching for ivory). Therefore, elephant ivory can only be traded with CITES permission, whereas mammoth ivory may be legally exported and manufactured. Problems arise from the fact that often mammoth ivory and elephant ivory are illegally mixed, and spurious certificates sometimes assure that products were manufactured from legal mammoth tusks when in fact they are crafted from illegal elephant ivory.

Till now, several techniques have been used to provide the key identifying features of elephantine and mammoth ivory: optical microscopy (Brown and Moule, 1977; Banerjee et al., 2004; 2007; Rolandi, 1999; Trapani and Fisher, 2003), scanning electron microscopy (SEM) and transmission electron microscopy (TEM) (Banerjee et al., 2004, 2007), X-ray powder diffraction (Banerjee et al., 2004, 2007), X-ray fluorescence (Kautenburger et al., 2004), X-ray tomography (Enzmann et al., 2004, 2007), FT-IR spectroscopy (Banerjee et al., 2004, 2007), FT-Raman spectroscopy (Edwards et al., 1995, 1997, 2006; Banerjee, 2003, 2007), thermogravimetric analysis (Burragato et al., 1998), elemental analysis (ICP-AES and ICP-MS) (Singh et al., 2006), radiocarbon dating (Vasil'chuck et al., 1997).

We applied for the first time high resolution solid state magic angle spinning nuclear magnetic resonance (MAS NMR) spectroscopy for the characterization of both elephant and mammoth ivory. This technique was previously used to characterize the so-called "vegetable ivory" or ivory nut (*Phytelephas macrocarpa*) in order to enrich the solid-state structure models derived from diffraction methods (Marchessault et al., 1990).

By exploiting ^{1}H, ^{13}C and ^{31}P MAS NMR, the composition of several ivory specimens has been investigated. The multinuclear approach allows a detailed description of the nanostructured biomaterials from the point of view of the inorganic and organic phases. In particular, it provides a rich source of information about distances between the nuclei within the same nanophases and heterogeneous phases of hybrid structures. Solid state NMR spectroscopy could therefore be a useful tool for identifying and characterizing the possible environments of carbonate and hydroxide ions in biological apatites.

Elephant and mammoth ivory sources

Elephant ivory is derived from the only two species of family Elephantidae (order Proboscidea, class Mammalia, phylum Chordata) that survive today: *Loxodonta africana*, the African elephant, and *Elephas maximus*, the Asian or Indian elephant. Modern African and Indian elephants appear to have evolved in the Pleistocene and have remained relatively unchanged since then. The ivory-bearing tusks consist of two upper maxillary incisor teeth in both the male and the female African elephant, and the male, and sometimes the female, of the Asian elephant, as the female of this species has no or very small tusks. The long tapering tusks of both elephant species curve gently upwards and gradually taper towards their tips. Growth of dentin occurs in rhythmic layers from the outside inwards towards the pulp or nerve of the tusk. During dentin deposition, sets of odontoblasts (biological cells whose function is dentinogenesis) move in phase with each other and 180° out of phase with adjacent sets, producing alternating light and dark areas. The growth surface is progressively displaced towards the tusk axis and away from the cementum-dentin junction (Trapani and Fisher, 2003). Tusks grow continuously throughout life and when erupt they are covered by a thin layer of enamel which is quickly abraded by continuous use. Ivory varies in quality and weight with its geographical occurrence. Traditionally, the best ivory comes from Equatorial Africa (Brown and Moule, 1977).

Mammoth ivory is derived from the tusks of the so-called primitive elephants or woolly mammoths (*Mammuthus primigenius*) that belong to the same order (Proboscidea) and family (Elephantidae) as modern elephants. They are the most familiar of the elephant's extinct relatives. Mammoth had large slender upwardly curving tusks that were much more curved than those of the actual elephant. Preserved carcasses of these large mammals have been found in the 1,600,000 to 10,000 years old pleistocene sediments (permafrost) in the sub-arctic regions. They became extinct in the last glacial-interglacial cycle, between 12,000 and 10,000 years ago (Brown and Moule, 1977; Rolandi, 1999; Agenbroad, 2005). According to Stuart (1991, 1999), mammoth extinction in Alaska occurred prior to 12,500 BP. Mammoth extinction causes are still in great debate. Computer studies of their decline in numbers suggest that their extinction might be due to a combination of overhunting by humans and changes in the climate. Several reports based on radiocarbon results proposed rapid warming and concomitant vegetation change as a possible cause for dramatic extinction of the large Pleistocene grazers. Nevertheless, according to Agenbroad (2005), any extinction model which does not include the factor of human predation is in error for North America.

Ivory surface texture

Tusks of both elephant and mammoth show a typical "engine turning" surface pattern (Figure 1) that is readly visible on cross-sections (lying perpendicular to the longitudinal axis of the tusk), which is claimed to be diagnostic for this ivory type. This identifying "engine turning" pattern, described by Bernard Schreger (1800) and by Richard Owen (1856), consists of rhomb shaped curvilinear lozenges created by the regular intersections of gentle arcs of alternating brownish and yellowish striae that have been termed in the gemmological literature "striae of Retzius" or the "Schreger lines", as proposed by Hanausek (Burragato et al., 1998).

Polarized light studies by Keil (1966) (Brown and Moule, 1977) have revealed that this surface texture is an optical effect caused by the reflection of light from the extremely fine fibres of the collagen protein, which are oriented in two distinct directions in the peritubular matrix (the

Figure 1. Characteristic "engine-turningd" surface pattern of elephantine ivory (from a necklace, the scale bar corresponds to 1 cm), showing criss-crossing continuous Schreger lines ("X" type) and obtuse intersection angles.

matrix surrounding each dentinal tubule). Light and dark regions forming the Schreger pattern are thought to be macroscopic manifestations of systematic shifts in undulatory pathways of dentinal tubules produced by odontoblasts. Schreger patterns have been classified in three categories (Trapani and Fisher, 2003) on the base of their qualitative appearance: 1) "X" type, or criss-crossing continuous lines, occurring in both dextral and sinistral directions; 2) "C" type, or rectangular light and dark areas resembling a checkerboard; 3) "V" type, or continuous lines where one direction is locally dominant.

Penniman (1952) noted that Schreger lines were finer and closer together in mammoth than in elephant ivory and deduced that these pattern differences were the result of the greater curvature of mammoth tusks.

From a gemological point of view it is often quite difficult to discriminate elephant ivory and mammoth ivory, particularly if the polished objects are of small size. However, when the intersection angles (Schreger angles) of "engine-turning" lines can be identified and measured, they are used to provide this differentiation. In elephantine ivory such angles are obtuse (about 124°), while in mammoth ivory they are acute (about 73°). In longitudinal sections, that is parallel to the growth direction of the tusks, the orientation of the collagen fibres is simply unidirectional and not identifying. Therefore the surface texture is characterized by a pattern of wavy longitudinal brownish and yellowish striae. A similar feature may be readly observed also in the ivory of other mammals, whereas the "engine-turning" patterning is unique to elephant and mammoth ivory.

Composition and structure of tooth dentin

As all mammalian teeth, the bulk of elephant and mammoth proboscidean tusks, which are the enlarged, ever-growing incisors, is made of dentin surrounding the pulp chamber. When the tusk erupts, dentin is covered by a thin layer of enamel, a collagen-free carbonated apatite (Veis, 2003), which is the hardest mammalian tissue at 6½ on Mohs scale. Enamel is white and inelastic

and it is quickly abraded by continuous use. Below the enamel, the complete length of the tusk is covered by a relatively thin layer of yellowish cellular cementum, a less calcified elastic tissue that more closely resembles bone, which helps attach the tusk to its bony socket (Brown and Moule, 1977).

Tooth dentin and dental cementum are biomineralized tissues, characterized by an heterogeneous organic/inorganic composition. The structural organic matrix is comprised essentially of a network of type I collagen fibrils. The designation "type I" collagen indicates that several different collagens exist (Veis, 2003 and references therein). In fact, more than 40 vertebrate genes have been identified as members of the collagen protein family (Pace et al., 2003). Type I collagen belongs to the class of fibrillar collagens, which are all characterized by a long uninterrupted triple helix of polipeptide chains containing 300 or more $(GXY)_n$ amino acid sequence domains (where G is Glycine while X and Y may be any amino acid). Many studies have shown that a collagen fibril matrix by itself does not have the capacity to induce mineralization from a solution of calcium and phosphate ions at the appropriate PH, degree of saturation and temperature. The matrix-regulated models of mineral induction place the focus of mineral nucleation on the presence of "accessory" proteins with the ability to induce the nucleation of the mineral deposition (Lowenstam, 1981; Veis, 2003 and references therein). In general, the dentin and cementum proteins are acidic in nature. The set of acidic mineralized tissue matrix proteins belong to the SIBLING (Small Integrin-Binding-Ligand-N-linked Glycoprotein) family (Fisher et al., 2001). The first to be identified was in dentin (Veis and Schlueter, 1963, 1964; Schlueter and Veis, 1964) and named "phosphophoryn" or phosphate carrier protein or PP. PP strongly binds to fibrillar collagen (Veis, 2003 and references therein) enhancing the ability of the fibril network to bind and retain calcium ions.

The inorganic part or mineral matrix of tooth dentin is constituted of biological apatites, which are Ca-deficient non-stoichiometric carbonated-hydroxyapatite with the general formula $Ca_{10-x}H_x(PO_4,CO_3)(OH)_{2-x}$ (Veis, 2003). In general the apatites have two types of anionic sites: the monovalent ones located in channels along the c-axis of the hexagonal structure, which are occupied by hydroxide, cloride or fluoride ions, and the trivalent ones in which the phosphate ions are located (Beshah et al., 1990). Bioapatites are in fact carbonated-hydroxyapatites with two kinds of substitutions occurring in the crystal lattice: CO_3^{2-} for OH^- (minor form, type A substitution) and CO_3^{2-} for PO_4^{2-} (major form, type B substitution) in percentage of 4-8%. (Kolmas et al., 2012). They contain also water molecules and various extraneous components (Mg^{2+}, Na^+, K^+, F^-, Cl^-), citrate or HPO_4^{2-} ions, located in the crystal lattice and on the crystal surface, which serves as interface between the mineral and the organic matrix. Palombo et al. (2005) reported that there is a poor correlation between OH^- and CO_3^{2-}, indicating that the increase in CO_3^{2-} during fossilization (i.e. Mammoth) was mainly associated with an increased replacement of PO_4^{3-} by CO_3^{2-}. Moreover, Pasteris et al. (2001) (in Palombo et al., 2005) found that, as OH^- decrease and CO_3^{2-} increase, the degree of crystallinity of the apatite decreases.

Small dimensions, low cristallinity, non-stoichiometric composition, inner crystalline disorder and presence of other ions in the crystal lattice are distinct features of biological apatites. It was demonstrated from electron microscopic and X-ray diffraction studies that crystals of apatite within dentin matrix are small and plate or needle-like in shape, with the longer axis parallel to the c-axis of the bioapatite hexagonal cell (Banerjee et al., 2004, 2007), and they are oriented so that the c-axes are near parallel with the collagen fibril axis (Veis, 2003).

Materials and Methods

Samples

We analyzed five specimens of African elephant ivory, taken from necklace beads and jewellery objects, two specimens of Asian elephant ivory, taken from tusks of a female elephant, five specimens of mammoth ivory from Siberia (three specimens from rough material, one specimen from a carved piece and one specimen from a cabochon-cut piece). All specimens have been manually powdered in an agate mortar to keep unchanged the crystalline structure.

X-ray powder diffraction

X-ray diffraction has been performed using a Bruker D8 diffractromer in the Bragg-Brentano geometry. The radiation wavelength of the incident X-rays was 1.5406 Å and a 2θ range from 10° to 60° was investigated.

MAS NMR Spectroscopy

^{1}H, ^{13}C and ^{31}P MAS NMR spectra were run at 300 MHz, 75.5 MHz and 121.5 MHz, respectively, on a Bruker Avance 300 MHz instrument operating at a static field of 7.04 T. A MAS Bruker probe head was used with 4 mm ZrO_2 rotors spinning at the speed of 15 kHz. Cross-polarization times of 0.5 ms were applied on each sample in ^{13}C CP-MAS NMR measurements. Quantitative ^{1}H MAS NMR measurements have been performed by using a recycle delay of 20 s. Quantitative ^{31}P MAS NMR measurements have been performed by using a recycle delay of 500 s.

Spectral profiles were fit by Lorentzian line shapes for the ^{1}H spectra, while ^{31}P spectra were simulated by Gaussian-Lorentzian functions (xG/(1-x)L = 0.5).

Results

X-ray powder diffraction

The XRD patterns of both elephant and mammoth ivory samples correspond to the standard apatite crystal structure (Figure 2). No additional peaks from other crystalline calcium phosphates have been identified, according to Kolmas et al. (2012). A low crystallinity can be deduced from broad peaks shown by diffraction patterns in all analyzed samples. Nevertheless,

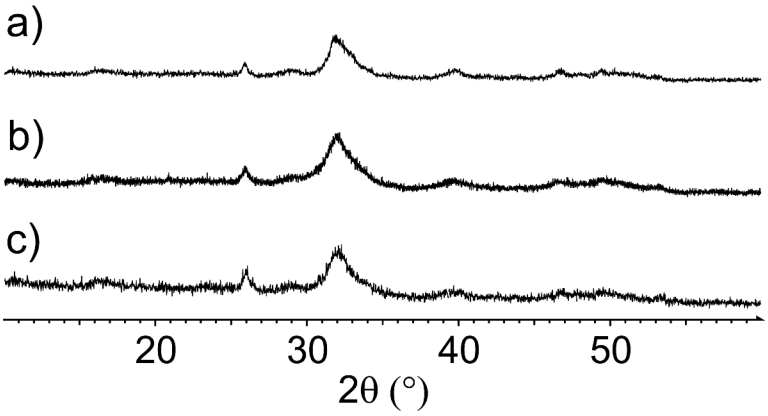

Figure 2. Powder X-ray diffraction patterns of: a) African Elephant 1; b) Rough Mammoth 1; c) Rough Mammoth 3.

mammoth ivory shows broader peaks, indicating a lower grade of crystallinity, due to an increase of CO_3^{2-} in the partially fossilized material. These results agree with those obtained by Raman spectra, where the CO_3^{2-} mode (1070 cm^{-1}) in carbonated hydroxy-apatite is significantly more intense in mammoth than in elephant ivory (Edwards et al.,1997).

It has been stated that the poor crystallinity of the XRD patterns is caused mainly by the tiny dimensions of the crystallites. "Because the degree of anisotropy by average crystallite size is much bigger than the average maximum strain, i.e. structure imperfections, it can be concluded that the crystallite size is the main reason for the apatite reflection broadening" (Banerjee et al., 2004, 2007).

MAS NMR Spectroscopy

Solid State NMR spectroscopy provides important information on organic matrix, carbonates and intracrystalline apatite hydroxyls, which cannot be obtained any other way (Kolmas et al., 2012). The ^{13}C CP-MAS NMR spectra of elephant (both African and Asian) and of mammoth ivory present two regions of interest (Figure 3): the 0-70 ppm region, characteristic for amino acid residues, and that around 170 ppm, specific for both carbonyl groups of the organic matrix and for apatite

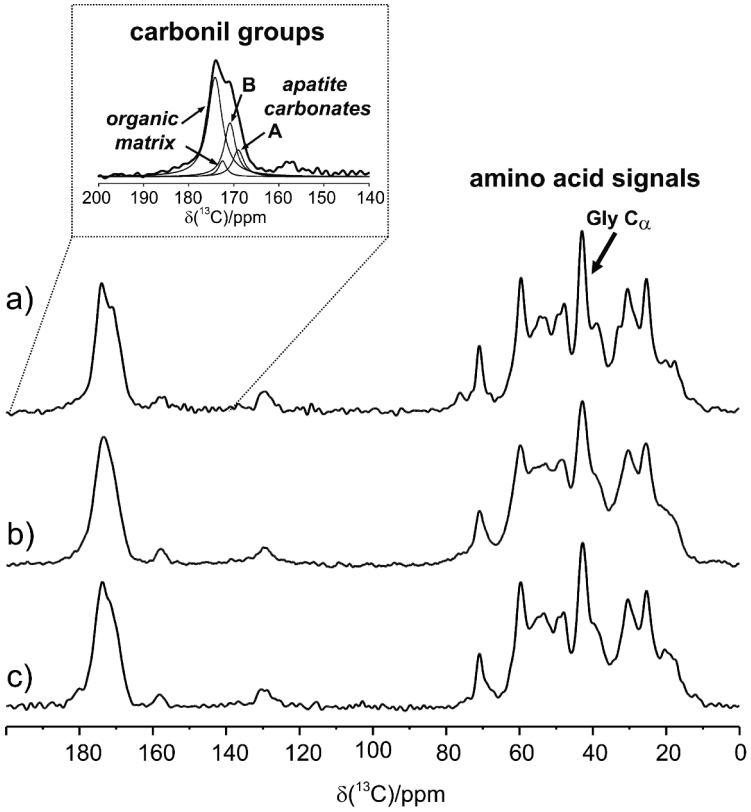

Figure 3. ^{13}C CP MAS spectrum performed with a contact time of 0.5 ms and a spinning speed of 15 kHz of a) African Elephant 1, b) Asian Elephant 2 and c) Rough Mammoth 1.

carbonates. Both elephant and mammoth ivory spectra show main peaks with the same chemical shifts and analogous intensity ratios; slightly narrower peaks have been observed in African elephant ivory. Features in the 0-70 ppm region can be assigned to collagen type I with the typical predominant peak at 42.5 ppm from Cα of glycine. Furthermore, the ^{13}C CP-MAS NMR experiments allowed the identification of carbonate groups from apatite in all specimens (Comotti et al., 1996). The broad organic carbonyl signals at about 174 ppm contain additional peaks at ca. 170 and 168 ppm assigned to the carbonates of the inorganic matrix, which may respectively be assigned to type B apatite and to type A apatite (according to Kolmas et al., 2012).

The existence of CO_3^{2-} - OH or CO_3^{2-} - H_2O complexes has been suggested in which the OH^- ion or the H_2O molecule may occupy the oxygen vacancy left by the substitution of PO_4^{3-} with CO_3^{2-}.Associations of CO_3^{2-} with a hydroxide ion have been observed in carbonate hydroxyapatite. Therefore, several OH^- locations may also exist in carbonate apatite. In order to identify such associations, a ^1H NMR investigation was performed, which gave more information on the apatite structure groups. In the proton spectra of both elephant and mammoth ivory a sharp resonance at 0.0 ppm from structural hydroxyl groups (Figure 4) of apatite was observed. There are sharp resonance peaks at 0.9 and 1.3 ppm, mainly from the organic matrix. The broad massive signal at 4.8-4.9 ppm has been assigned to surface water (Kolmas et al., 2012). The

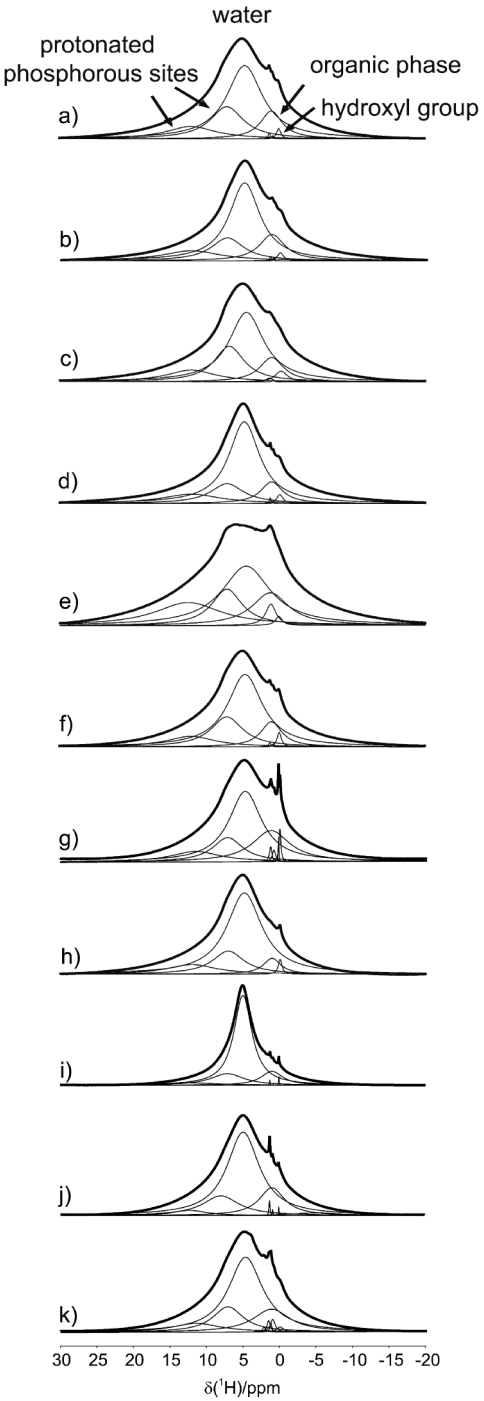

Figure 4. Quantitative ^1H MAS NMR spectra recorded at 300 MHz by using a spinning speed of 15 kHz and 20 s recycle delay of: a) Rough Mammoth 1; b) Rough Mammoth 2; c) Rough Mammoth 3; d) Cabochon-cut Mammoth; e) Carved Mammoth; f) Asian Elephant 1; g) Asian Elephant 2; h) African Elephant 1; i) African Elephant 2; j) African Elephant 3; k) African Elephant 4.

signals were quantified by the deconvolution analysis and the results indicate that mammoth ivory presents a lower amount of water than African and Asiatic elephant ivory. Similar results have been obtained by Yin et al. (2013) with Infrared Spectroscopy analysis. The NMR spectrum of the carved mammoth ivory shows broad peaks connected to the presence of paramagnetic impurities (Figure 4e) probably due to the carving technique.

^{31}P MAS NMR spectra of both elephant and mammoth ivory produce peak maxima around 3 ppm as expected from their common calcium orthophosphate structural content (Figure 5). The NMR response from both ivory types features a narrow Lorentzian peak, which reflects an ordered crystal structure. The simulation procedure shows the major signal at ca. 3.0 ppm overlapped with two minor signals (Figure 5a) at about 0.8 ppm and at about 6 ppm, respectively assigned to protonated surface sites PO_xH and to unprotonated surface sites PO_x (PO, PO_2^- and PO_3^{2-}) (Jarlbring et al., 2006). In the Rough Mammoth 1 sample a narrow side peak at 6.3 ppm can be noticed (Figure 5a), which may be an indication of another type of phosphorous sites or a contribution from active surface sites of phosphorous.

Conclusions

In this work ^{13}C CP-MAS NMR, ^{1}H and ^{31}P MAS NMR spectroscopy were applied for the first time to characterize elephant and mammoth ivory. The purpose was to provide a diagnostic technique to discriminate between elephant and

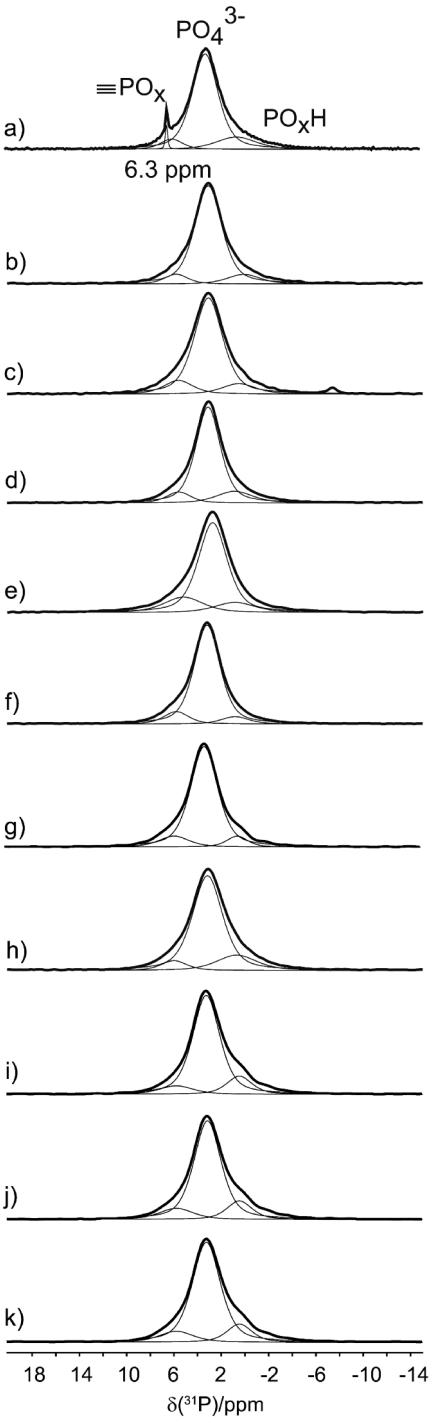

Figure 5. Quantitative ^{31}P MAS NMR spectra of: a) Rough Mammoth 1; b) Rough Mammoth 2; c) Rough Mammoth 3; d) Cabochon-cut Mammoth; e) Carved Mammoth; f) Asian Elephant 1; g) Asian Elephant 2; h) African Elephant 1; i) African Elephant 2; j) African Elephant 3; k) African Elephant 4.

mammoth ivory types.

The most important results of this study can be drawn as follows:

- ^{13}C CP-MAS NMR spectra showed the presence of fibrous (type I) collagen in the organic matrix and of type B and type A carbonates from apatite in all specimens. The apatite structure of the orthophosphate was confirmed by X-ray powder diffraction. Elephant's and mammoth's ivory mineral matrix should therefore be classified as carbonated hydroxyapatite of mixed type AB. No substantial differences in signal chemical shifts have been highlighted between elephant and mammoth ivory. Larger line-width have been observed in Asian elephant and mammoth ivory spectra, but they cannot be considered a diagnostic evidence.

- ^{1}H MAS NMR spectra evidenced the presence of structural hydroxyl groups, of proton sites and of surface water in both ivory types, probably indicating an interaction of protons associated to carbonate ions and water molecules.

- Resonance lines in ^{31}P MAS NMR spectra confirmed the presence of calcium orthophosphate or (bio)apatite, of protonated and unprotonated surface sites in both elephant and mammoth ivory types.

Taken into consideration the above mentioned results, at the moment the MAS NMR spectroscopy by itself should not be considered a completely diagnostic technique to differentiate between elephant and mammoth ivory. The more or less resolution of some spectroscopic bands assigned to the collagen component can give indications, but it is not a powerful tool. Nevertheless, from a qualitative point of view, it should be underlined that no substantial differences have been highlighted in the mineral phase and in the amino acid composition of elephant and mammoth ivory. Therefore the MAS NMR spectroscopy can be useful to characterize both ivory types and to discriminate between ivory and ivory substitutes. Moreover, it is a destructive technique and therefore unlikely to be applied to artefacts of gemmological and hystorical importance.

Acknowledgements

Authors are grateful to:

- dr. Giorgio Bardelli, Museum of Natural History, Milano, for specimens of Asian elephant ivory;

- Gianmaria Buccellati, honorary president of Istituto Gemmologico Italiano, Milano, for specimens of African elephant ivory.

- dr. Alice Silvia Cattaneo, University of Milano - Bicocca, Dept. of Materials Science, for some NMR experiments;

- Romano Marini, Orient Express, Badia Tebalda (AR), for specimens of Mammoth ivory.

- The authors thank the referee Maurizio Paci and an anonimous referee for helpful suggestions.

References

Agenbroad L.D. (2005) - North American Proboscideans: mammoths: the state of knowledge, 2003. *Quaternary International*, 126-128, 73-92.

Banerjee A., Bortolaso G. and Dindorf W. (2004-2007) - Distinction between African and Asian ivory. In: Elfenbein und Artenschutz, Proceedings of INCENTIVS, Mainz University, 37-49.

Banerjee A., Bortolaso G., Hofmeister W., Petrovic-Prelevic I. and Kiewisch B. (2004-2007) - Investigation of quality of commercial mammoth ivory by means of X-ray powder diffraction (Rietveld method) and FTIR spectroscopy. In: Elfenbein und Artenschutz, Proceedings of INCENTIVS, Mainz University, 51-63.

Beshah K., Rey C., Glimcher M.J., Schimizu M. and Griffin R.G. (1990) - Solid state carbon-13 and proton NMR studies of carbonate-containing calcium phosphates and enamel. *Journal of Solid State Chemistry*, 84, 71-81.

Brown G. and Moule A.J. (1977) - The structural characteristics of various ivories. *Australian Gemmologist*, 13, 47-60.

Burragato F., Materazzi S., Curini R. and Ricci G.

(1998) - New forensic tool for the identification of elephant or mammoth ivory. *Forensic Science International*, 96, 189-196.

Comotti A., Simonutti R. and Sozzani P. (1996) - Hydrated calcium silicate and poly(vinyl alcohol): Nuclear Spin propagation across heterogeneous interfaces. *Chemistry of Materials*, 8, 2341-2348.

Edward H.G.M., Brody R.H., Hassan N.F.N., Farwell D.W. and O'Connor S. (2006) - Identification of archaeological ivories using FT-Raman spectroscopy. *Analytica Chimica Acta*, 559, 64-72.

Edwards H.G.M. and Farwell D.W. (1995) - Ivory and simulated artefacts: Fourier-transform Raman diagnostic study. *Spectrochimica Acta*, Part A, 51, 2073-2082.

Edwards H.G.M., Farwell D.W., Holder J.M. and Lawson E.E. (1997) - Fourier-transform Raman spectroscopy of ivory II: spectroscopic analysis and assignments. *Journal of Molecular Structure,* 435, 49-58.

Edwards H.G.M., Farwell D.W., Holder J.M. and Lawson, E.E. (1997) - Fourier-transform Raman spectroscopy of ivory III: identification of mammalian specimens. *Spectrochimica Acta*, Part A, 53, 2403-2409.

Enzmann F., Kersten M., Goebbels J. and Meinel D. (2004-2007) - High-resolution X-ray tomography imaging of ivory. In: Elfenbein und Artenschutz, Proceedings of INCENTIVS, Mainz University, 81-86.

Fisher L.W., Torchia D.A., Fohr B., Young M.F. and Fedarko N.S. (2001) - Flexible structures of SIBLING proteins, bone sialoprotein, and osteopontin. *Biochem Biophys Res Commun*, 280, 460-465.

Jarlbring M., Sandström D.E., Antzutkin O.N. and Forsling W. (2006) - Characterization of active phosphorus surface sites at synthetic carbonate-free fluoapatite using single-pulse 1H, 31P, and 31P CP MAS NMR. *Langmuir*, 22, 4787-4792.

Kautenburger R., Wannemacher J. and Müller P. (2004) - Multi element analysis by X-ray fluorescence: A powerful tool of ivory identification from various origins. *Journal of Radioanalytical and Nuclear Chemistry*, 260, 2, 399-404.

Kolmas J., Szwaja M. and Kolodziejski W. (2012) - Solid-state NMR and IR characterization of commercial xenogenic biomaterials used as bone substitutes. *Journal of Pharmaceutical and Biomedical Analysis*, 61, 136-141.

Lowenstam H.A. (1981) - Minerals formed by organisms. *Science*, 211, 1126-1131.

Marchessault R.H., Taylor M.G. and Winter W.T. (1990) - ^{13}C CP/MAS NMR spectra of poly-β-D(1→4) mannose: mannan. *Canadian Journal of Chemistry*, 68(7), 1192-1195.

Owen R. (1856) - On the ivory and teeth of commerce. *Journal of Royal Society of the Arts*, 5, 65-71.

Pace J.M., Corrado M., Missero C. and Byers P.H. (2003) - Identification, characterization and expression of a new fibrillar collagen gene, COL27A1. *Matrix Biology*, 22, 3-14.

Palombo M.R., Filippi M.L., Iacumin P., Longinelli A., Barbieri M. and Maras A. (2005) - Coupling tooth microwear and stable isotope analyses for paleodiet reconstruction: the case study of late Middle Pleistocene Elephas (Paleoloxodon) antiquus teeth from Central Italy (Rome area). *Quaternary International*, 126-128, 153-170.

Pasteris J.D., Wopenka B., Freeman J., Rogers K.D., Valsami-Jones E. and VanDerHouwen J.A.M. (2001) - Apatite in bone is not hydroxylapatite: there must be a reason. The Geological Society of America Annual Meeting, 5-8, 158 (Abstract).

Penniman T.K. (1952) - Pictures of ivory and other animal teeth, bone, and antler. *Pitt Rivers Museum Occasional Papers on Technology*, 5, 1-37.

Rolandi V. (1999) - Characterisation of recent and fossil ivory. *Australian Gemmologist*, 20, 266-276.

Schlueter R.J. and Veis A. (1964) - The macromolecular organization of dentin matrix collagen. II. Periodate degradation and carbohydrate cross-linking. *Biochemistry*, 3, 1657-1665.

Schreger B.N.G. (1800) - Beitrag zur Geschichte der Zähne. *Beitrage für die Zergliederungkunst*, 1, 1-7.

Singh R.R., Goyal S.P., Khanna P.P., Mukherjee P.K. and Sukumar R. (2006) - Using morphometric and analytical techniques to characterize elephant ivory. *Forensic Science International*, 162, 144-151.

Stuart A.J. (1991) - Mammalian extinctions in the late Pleistocene of northern Eurasia and North America. *Biological Review*, 66, 453-562.

Stuart A.J. (1999) - Late Pleistocene megafaunal extinctions: a European perspective. In: Macphee R.D.E. (Ed.), Extinctions in near time: causes, contexts, and consequences. Kluwer Academic/Plenum, New York, 257-270.

Trapani J. and Fisher D.C. (2003) - Discriminating Proboscidean taxa using features of the Schreger pattern in tusk dentin. *Journal of Archaeological Science*, 30, 429-438.

Vasil'chuck Y., Punning J-M. and Vasil'chuck A. (1997) - Radiocarbon ages of mammoths in northern Eurasia: implications for population development and late Quaternary environment. *Radiocarbon*, 39, 1-18.

Veis A. (2003) - Mineralization in organic matrix frameworks. In: Dove, P.M., De Yoreo J.J. and Weiner S. (eds): *Reviews in Mineralogy & Geochemistry- Biomineralization*, 54, 249-289.

Veis A. and Schlueter R. J. (1963) - Presence of phosphate-mediated cross-linkages in hard tissue collagens. *Nature*, 197, 1204.

Veis A. and Schlueter R.J. (1964) - The macromolecular organization of dentin matrix collagen. I. characterization of dentin collagen. *Biochemistry*, 3, 1650-1656.

Yin Z., Zhang P., Chen Q., Zheng C. and Li Y. (2013) - A comparison of modern and fossil ivories. *Gems & Gemology,* 49, 1, 16-27.

Submitted, February 2013 - Accepted, May 2013